Journal of Membrane Science 446 (2013) 59–67

Contents lists available at SciVerse ScienceDirect

Journal of Membrane Science

journal homepage: www.elsevier.com/locate/memsci

Generating backwashable carbon nanotube mats on the inner surface of polymeric hollow fiber membranes

M.J. Gallagher [a], H. Huang [b], K.J. Schwab [b], D.H. Fairbrother [a], B. Teychene [c,*]

[a] Department of Chemistry, Johns Hopkins University, Baltimore, MD 21218, USA
[b] Department of Environmental Health Sciences, Johns Hopkins University Bloomberg School of Public Health, Baltimore, MD 21205, USA
[c] Institut de Chimie des Milieux et des Matériaux de Poitiers (IC2MP; UMR: 7285), Université de Poitiers, 1 rue Marcel Doré, Bâtiment 16, 86022 Poitiers Cedex, France

ARTICLE INFO

Article history:
Received 1 February 2013
Received in revised form
14 May 2013
Accepted 11 June 2013
Available online 21 June 2013

Keywords:
Carbon nanotube
Hollow fiber
Backwashable mats
Water purification

ABSTRACT

Porous carbon nanotube (CNT) mats adsorbed on flat sheet membranes have previously been shown to significantly improve fouling resistance and contaminant removal capabilities. Unfortunately, these CNT mats are easily disrupted by backwashing, severely limiting their value in commercial membranes. In this study, we describe how CNT mats, which are stable to backwashing, can be generated on the inner surface of hollow fiber membranes. Mat stability was determined from electron microscopy and by quantifying the mass of CNTs lost during aggressive backwashing, including hydraulic stress and exposure to harsh chemicals. Stable mats were also formed with powder activated carbon, demonstrating that the mat's stability is not a consequence of CNT properties, but rather the nature and directionality of the forces that these mats experience during backwashing. Compared to virgin membranes, CNT-modified membranes exhibited improved fouling resistance which was sustained through multiple backwashing cycles. Moreover, no measureable quantities of CNTs entered the permeate when natural organic matter was filtered through a CNT-modified membrane, indicating that CNTs will not be released into the permeate during filtration. Collectively, these findings indicate that CNT-modified membranes could positively impact the sustainability and performance of hollow fiber membranes being used in water purification.

1. Introduction

In the past decade, the unique physicochemical properties of nanomaterials, such as nano-silver, nano-scale metal oxides and carbon nanotubes (CNTs), has enabled significant breakthroughs to be realized in numerous fields, including commercial products, analytical tools, water purification, and medicine [1–5]. CNTs are particularly well suited to positively impact water treatment as transformative components in the design of new nano-enabled environmental technologies based on separation processes (adsorption, filtration, etc.) [6,7]. In part, this interest in CNTs is driven by their extremely high surface area-to-volume ratios making them attractive candidates as a new class of carbon-based sorbents for chemical and microbial removal from water [8–14]. Thus, CNTs are effective at removing hydrophobic organic chemicals [15–17], heavy metals [18–22], natural organic matter [16] as well as viruses and bacteria [23–25]. The high surface area and conductivity also enables CNT mats to function as three dimensional porous electrodes. This has opened up the possibility of using redox reactions to destroy contaminants when they adsorb onto CNT mats, augmenting sorption as a means for contaminant removal [26–31]. For example, concomitant electrolysis during filtration through CNT mats was found to remove *E. coli* bacteria and MS2 viruses by more than 6-$\log_{10}$ [26]. In addition to contaminant removal, previous studies have shown microporous CNT mats, when attached to flat sheet membranes, enhance fouling resistance tripling the time for transmembrane pressure (TMP) to increase with minimal reduction in the membrane's clean water permeability [32]. This enhanced resistance to fouling has been ascribed to the ability of the CNT mat to trap species responsible for fouling [33].

Membranes modified by CNT mats clearly hold significant promise for improving the energy efficiency and sustainability of next generation membranes for water purification. Moreover, the commercial and economic viability of integrating CNTs into membranes has been made possible by increased demand and production [34]; kilogram quantities of CNTs can now be purchased for less than $1000. Unfortunately, mats created from pure CNTs on flat sheet membranes exhibit poor stability and cannot be easily handled or integrated into real world membrane systems

* Corresponding author. Tel.: +33 549453846.
E-mail address: benoit.teychene@univ-poitiers.fr (B. Teychene).

0376-7388/$ - see front matter © 2013 Elsevier B.V. All rights reserved.
http://dx.doi.org/10.1016/j.memsci.2013.06.015

[35]. This instability is a consequence of the large quantity of CNTs that are released from the membrane's surface and into the permeate during backwashing [32]. This release of CNTs not only greatly restricts their practical value, but also raises important health and safety concerns associated with the presence of CNTs in the treated water. Synthetic strategies have recently been used to chemically graft CNTs onto the surface of cellulose nitrate membranes, although only as a minor component (20% maximum) of a matrix containing poly(vinyl) alcohol and succinic acid [36].

This paper describes our recent discovery that mats composed exclusively of CNTs can be created with a simple preparative method on the internal surface of hollow fiber low pressure membranes, and that these mats remain structurally intact on the membrane's surface even after several backwashes and aggressive chemical cleaning. Hollow fiber, low pressure membranes (LPMs), such as polyvinylidene fluoride (PVDF) and polyethersulfone (PES) [37] are used for many types of water treatment strategies (except desalination) and can be operated in either an inside-out (active layer on the inner surface) or outside-in (active layer on the outer surface) configuration. LPMs act as a physical barrier for contaminant removal [38], removing aquatic constituents larger than membrane pores, such as algae, bacteria, and parasites. The removal of human enteric viruses (20–90 nm in diameter) by LPMs, however, is often incomplete as these small diameter viruses can pass through the larger diameter pores in LPMs. Additionally, LPMs cannot remove most dissolved substances with the exception of limited adsorption of some organic chemicals [39–42]. The discovery that backwashable CNT mats can be created by a simple methodology on the inner surface of hollow fiber membranes therefore opens up the possibility to exploit the benefits of CNT mats to enhance the performance of LPMs in real world applications.

2. Materials and methods

2.1. Base materials

Carbon nanotubes: Commercially available pristine (unfunctionalized) multiwalled CNTs (MWCNTs) were purchased from Cheap Tubes Inc. (Vermont, USA). According to the manufacturer's specifications, the MWCNTs exhibit diameters ranging from 50 to 80 nm and lengths between 10 and 20 μm and a specific surface area of 60 $m^2\ g^{-1}$. Prior to loading, MWCNT suspensions were prepared at an approximate concentration of 750 mg L^{-1} in Milli-Q water (18 MΩ cm^{-1}) with 0.9% v/v_{H_2O} of non-ionic surfactant (Triton X100). To help disperse the CNTs, all MWCNT suspensions were sonicated in a water bath sonicator for 30 min (Aquasonic 250HT).

Hollow Fiber Membranes: Two types of commercially available hollow fiber (HF) membranes were used: PES and PVDF. The PES membranes are hydrophilic with a nominal pore size of 0.03 μm and are capable of sustaining a maximum pure water flux of approximately 1200 ± 120 L $h^{-1}\ m^{-2}\ bar^{-1}$. The PVDF membranes are hydrophobic with a nominal pore size of 0.1 μm and are able to sustain a maximum flux of pure water of approximately 655 ± 85 L $h^{-1}\ m^{-2}\ bar^{-1}$.

Creating Membrane Modules: All filtration experiments were performed using the bench scale filtration system described in Huang et al. [43]. Virgin hollow fiber PES (HF-PES) and PVDF (HF-PVDF) membranes, ≈9.5 cm in length, were potted in epoxy with one end cut open to allow inside out, dead end filtration. The inner surface area of ≈9 cm^2 was kept consistent between different modules; four fibers for HF-PES and six for HF-PVDF modules. Once prepared the HF-PVDF and HF-PES membrane modules were soaked overnight in 25% v/v_{H_2O} isopropanol solution or Milli-Q water, respectively and then attached to the filtration system. Prior to each experiment the virgin module was flushed with Milli-Q water and the pure water flux measured by the flux step method [44]. A new membrane module was used for each experiment.

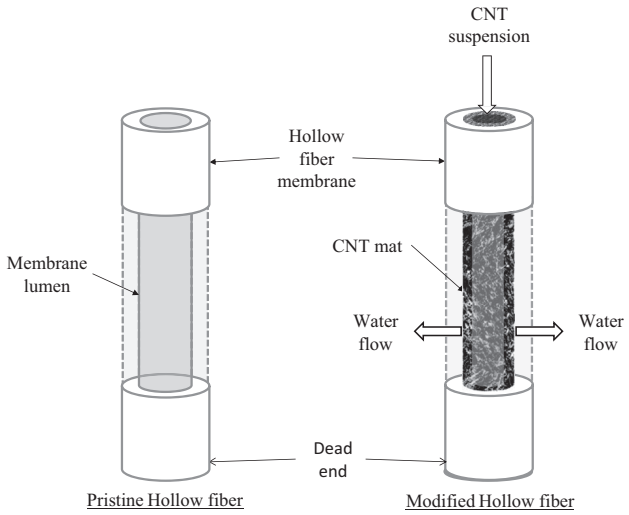

Fig. 1. Preparing a CNT mat by filtering a CNT suspension through a hollow fiber membrane from the "inside out". Membrane before loading (Left). Modified membrane (Right).

Fig. 1 summarizes the approach used to create CNT mats on the inner surface of virgin, HF-PES and HF-PVDF membranes. Hereafter, we refer to PES and PVDF hollow fiber membranes modified by the addition of CNT mats to their inner surfaces as HF-PES-CNT and HF-PVDF-CNT membranes, respectively. CNT mats were created by filtering 13 mL of a 750 mg L^{-1} CNT suspension through each hollow fiber module in an inside-out mode at a constant filtration flux of 134 L $h^{-1}\ m^{-2}$ using a peristaltic pump. The CNT loading was maintained at ≈11 g MWCNT m^{-2}. During the CNT loading process, the transmembrane pressure (TMP) was recorded every 10 s with a pressure transducer connected to an electronic board. The mat was created during the filtration process as CNTs were trapped on the inner surface of the hollow fibers. Once the CNTs had been loaded the residual surfactant was flushed from the module with Milli-Q water until the TMP reached a constant value. Once created the pure water flux passing through the HF-PES-CNT and HF-PVDF-CNT membranes was determined using Milli-Q water and the flux step method [44]. See Fig. S1 for a picture of a module during the formation of a HF-PVDF-CNT membrane.

The CNT loading (mg MWCNT m^{-2}) was determined by multiplying the MWCNT concentration (mg L^{-1}) by the total volume of MWCNT-containing solution filtered through the hollow fibers. This enabled us to calculate the total mass of MWCNTs (mg) used during the loading process. This value was then divided by the inner surface area of the HF-PVDF or HF-PES modules (m^2) to obtain the CNT loading (mg MWCNT m^{-2}).

2.2. Evaluating the stability of CNT mats towards backwashing

Once the CNT mats were created, mat stability was evaluated by reversing the flow of water through HF-PES-CNT and HF-PVDF-CNT membranes using hydraulic backwashing, i.e. outside-in flow. Three different backwash conditions were applied in sequence: (i) long term (2 h) backwashing with Milli-Q water at 85 L $h^{-1}\ m^{-2}$, (ii) hydraulic stress with Milli-Q water for 3 min at four increasing fluxes ranging from 85 to 420 L $h^{-1}\ m^{-2}$; each step was performed by flux pulsation (the flux was increased instantaneously and not incrementally) and, (iii) chemical stress involving three sequential (3 min) backwashing steps at 85 L $h^{-1}\ m^{-2}$ performed with three different chemicals in Milli-Q water: (a) synthetic surface water (49 ppm $NaHCO_3$, 28 ppm $CaSO_4$, 25 ppm $MgSO_4$ and 1.9 ppm KCl),

(b) 5 ppm and 500 ppm sodium hypochlorite solutions and, (c) a non-ionic surfactant suspension (0.9% v/v_{H_2O} Triton-X). The (i), (ii), (iii) sequence of backwashing steps was performed in triplicate, i.e. on three HF-PES-CNT and three HF-PVDF-CNT modules. Compared to normal membrane operation the backwashing conditions used in this study to test the stability of the CNT mats represent worst case scenarios in terms of duration, flux and chemical reagents. For the long backwash step (i) a 3 ml aliquot of backwashed water was collected every 10 min. For each of the steps described in backwash steps (ii) and (iii) a 3 ml aliquot of the backwashed water sample was collected.

The mat's stability during each backwashing step was assessed by determining the mass of CNTs dislodged from the mats. This was done by analyzing the concentration of MWCNTs in the backwashed water using UV–vis Spectroscopy (UV–vis). To determine the MWCNT concentration (and thereby the mass of CNTs released during each backwash step) by UV–vis it is necessary to ensure that all of the CNTs are dispersed. This was accomplished by first adjusting the pH of the backwash water to 10, as we have shown previously that high pH improves CNT dispersion [45]. Following this step, 0.5% v/v_{H_2O} of the surfactant Triton X100 was added to the solution and sonicated at 70 W (Branson 1510) for ≈15 min. The CNT concentration was then determined by measuring the average UV absorbance in the 800–900 nm range where control studies (see Fig. S2) showed that Triton X100 does not absorb but MWCNTs absorb/scatter light. The sensitivity of these measurements was enhanced by using a 5 cm path length UV–vis cell. The correlation between UV absorbance in the 800–900 nm range and MWCNT mass concentration (mg L^{-1}) was determined by conducting separate control studies where known masses of MWCNT powders were dispersed in Milli-Q with 0.5% Triton X100 v/v_{H_2O} (see Fig. S3). Using this information, the CNT mass released from the mat in any backwash step could be determined by multiplying the CNT mass concentration, determined by UV–vis, by the total sample volume collected during backwashing.

The limit of MWCNT detection was determined by identifying the lowest UV–vis absorbance value that could visibly be discerned from the baseline (0.011 absorbance units). A range of uncertainty in the MWCNT detection limit was then calculated from the uncertainty in the calibration curve shown in Fig. S3. Based on this analysis we estimate that the limit of MWCNT detection lies between 2.5–6.6 $\times 10^{-5}$ mg MWCNT.

2.3. Evaluation of CNT release into the permeate during NOM filtration

During membrane operation organic matter passing through the membrane could remobilize CNTs from the mats and transport these CNTs through the hollow fiber membranes and into the permeate. To evaluate this possibility Suwannee River Natural Organic Matter (SRNOM) was used; a type of NOM that has been used extensively in previous membrane studies [46,47]. The SRNOM suspension was prepared at a concentration of 5 mg L^{-1}SRNOM, diluted in synthetic surface water (see Section 2.2), and filtered through a HF-PVDF-CNT module at 67 L h^{-1} m^{-2} in two 60 min cycles. In between these two cycles, the HF-PVDF-CNT membrane was backwashed with the permeate at 85 L h^{-1} m^{-2}. To test the possible mobilization of CNTs during this filtration processes the CNT concentration in the permeate was determined by the method described in Section 2.2, also taking advantage of the fact that NOM does not adsorb in the 800–900 nm region (see Fig. S4). The same approach was used to determine the CNT concentration during backwashing.

2.4. Effect of CNT mats on membrane antifouling properties

The fouling behavior of HF-PVDF-CNT and HF-PES-CNT membranes, including the effect of backwashing, was compared to virgin HF-PVDF and HF-PES membranes by measuring the change in TMP during the filtration of sodium alginate. In these studies, sodium alginate was chosen as a fouling surrogate for NOM rather than SRNOM because it has higher fouling potential [46,48,49] due to the presence of larger concentrations of higher weight macromolecules. Consequently, the filtration of alginate leads to membrane fouling on an accessible experimental time scale. In these studies an alginate suspension (5 ppm sodium alginate diluted in 47 ppm $NaHCO_3$ and 380 ppm KCl) was prepared at pH 7. This alginate suspension was filtered through HF-PVDF, HF-PES, HF-PVDF-CNT, and HF-PES-CNT membranes in dead-end mode at a constant flux of 67 L h^{-1} m^{-2} through four cycles each of 80 min duration with each filtration cycle followed by 6 min of backwashing with the permeate at 85 L h^{-1} m^2. Thus, the net permeate volume was equal to 90% of the feed water volume. Membrane fouling was evaluated by measuring the rate of TMP increase ($d(P_t-P_0)/dt$) vs. time during each filtration cycle, where P_0 is the initial TMP prior to the filtration of the alginate solution and P_t is the TMP at time t. The irreversible fouling was determined after each backwashing step by the pressure increase (ΔP) measured at the beginning of the subsequent filtration cycle.

2.5. SEM imaging of CNT mats

The inner surfaces of HF-PVDF-CNT and HF-PES-CNT membranes were imaged using a cold cathode field emission scanning electron microscope (JEOL 6700F, FESEM) with 1.0 nm resolution at 15 keV. Images were acquired after CNT loading and then again after the various backwashing steps (see Section 2.2) had been performed. Prior to analysis each membrane sample was dried for 48 h at room temperature. Cross-sectional images were taken by first cryo-snapping the membranes in the presence of liquid nitrogen and then sputter-coating them with platinum to prevent charging during SEM. Samples were mounted vertically onto the side of a sample stub and imaged at various magnifications.

3. Results and discussion

3.1. Preparation and characterization of CNT mats

Fig. 2 shows the change in TMP observed during the creation of three HF-PVDF-CNT (Fig. 2–A, left) and three HF-PES-CNT (Fig. 2-B, right) membranes. As the MWCNT suspension was being filtered through the membranes (Stage 1), the TMP increased rapidly, reaching a maximum after ≈6 min of filtration time. During Stage 1, the average TMP increase is higher for the HF-PVDF membranes (≈0.9 bars) than for the HF-PES membranes (≈0.5 bars). This difference between the two types of hollow fiber membranes is consistent with the hypothesis that the TMP increase during Stage 1 is predominantly a result of hydrophobic interactions between the base membrane and the surfactant present in the feed solution [50]. Stronger interactions (and thus greater changes in the TMP) would be expected between the hydrophobic segments of the surfactant and the hydrophobic HF-PVDF membranes as compared to the more hydrophilic HF-PES membranes [50].

Once the volume of the MWCNT suspension filtered through the membrane reached the desired MWCNT mass loading (≈13 ml based on the MWCNT concentration), the MWCNTs suspension was replaced by Milli-Q water (Stage 2). At this point, Fig. 2 shows that for both HF-PVDF-CNT (Fig. 2-A) and HF-PES-CNT (Fig. 2-B) membranes, the TMP decreased rapidly as the surfactant was flushed from the membrane. After approximately 40 min of washing with Milli-Q water, the TMP in all of the membranes remained roughly constant at values that were either comparable to or slightly higher than those of the virgin hollow fiber membranes. For the HF-PVDF-CNT and HF-PES-CNT membranes the

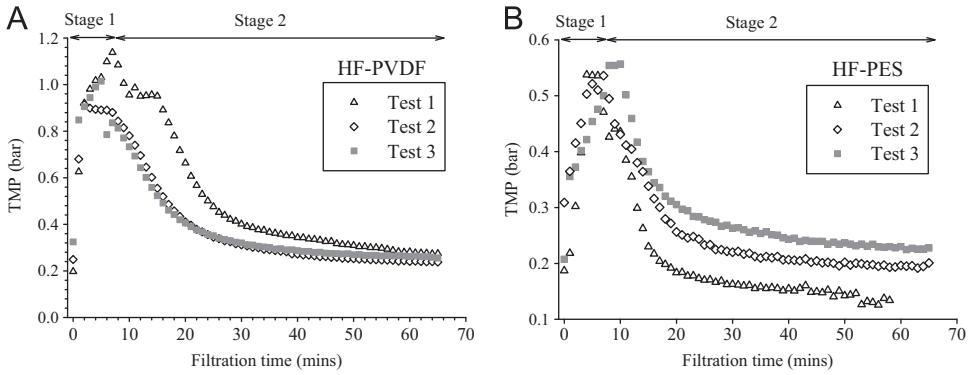

Fig. 2. Variation in TMP (bar) vs. Filtration time (min) during the preparation of MWCNT mats on the inner surface of HF-PVDF (A) and HF-PES (B) hollow fiber membranes. Stage 1: Filtration of the MWCNT suspension through the membrane from the "inside out". Stage 2: Filtration of Milli-Q water through the membrane following MWCNT loading.

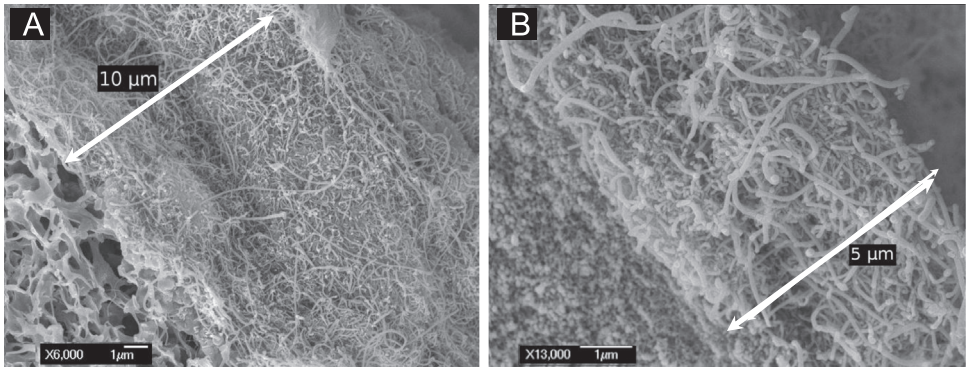

Fig. 3. SEM images of CNT mats created on the inner surface of (A) PVDF and (B) PES hollow fiber membranes. The white arrows show the mat depth on each membrane (depth corresponding to 11 g m^{-2} mass loading).

permeabilities were 500 ± 68 and 1080 ± 200 L h^{-1} m^{-2} bar^{-1}, respectively. In contrast, the permeability of the virgin HF-PVDF and HF-PES membranes were 655 ± 85 L h^{-1} m^{-2} bar^{-1} and 1200 ± 120 L h^{-1} m^{-2} bar^{-1}, respectively. Thus, the presence of CNT mats inside the hollow fibers reduces the membranes' permeability by approximately 22% for HF-PVDF-CNT and 10% for HF-PES-CNT membranes, respectively. These relatively small changes in permeability suggest that the CNT mats possess a large porosity and thus a low hydraulic resistance as compared to the base membrane.

SEM analysis of both HF-PVDF-CNT and HF-PES-CNT membranes (Fig. 3) confirms that the loading procedure creates a hybrid membrane with micron thick CNT mats, respectively, adsorbed on the inner surface of the hollow fiber. SEM images also reveal that the interface between the CNT mat and the base membrane is relatively sharp and well defined with little or no evidence of CNTs within the pores of either the HF-PVDF or HF-PES membranes. Based on the membrane's pore size (0.1 and 0.03 μm for the HF-PVDF and HF-PES, respectively), compared to the CNT geometry (O.D > 50 nm, length:10–20 μm), a total rejection of CNTs by the membrane during loading is expected. However, in previous studies we observed that MWCNTs (O.D: 10–20 nm, length:10–20 μm) dispersed by Triton-X100 permeated through flat sheet PVDF membranes with significantly higher pore size (≈0.45 μm) when vacuum filtration was used [32]. Thus, it appears that the properties of the support membrane and the details of the CNT filtration process are important in determining if a discrete CNT mat will be formed or not.

3.2. Evaluation of MWCNT mat's stability during backwashing

The stability of the three HF-PVDF-CNT and HF-PES-CNT membranes towards the aforementioned backwashing and cleaning conditions described in Section 2.2 were analyzed using UV–vis spectrometry, and the results are shown in Fig. 4. During long term backwashing with Milli-Q water the only measureable quantity of CNTs removed from any of the membranes occurred during the beginning of the backwash (< 10 min). This observation suggests that the CNTs displaced at the onset of the backwashing correspond to loosely bound aggregates of CNT particles, not well dispersed during sonication, that were only weakly adhered to the CNT mats. We hypothesize that this small fraction of weakly adhered CNTs is a consequence of the high CNT concentrations in the suspensions used to create the mats (750 mg L^{-1}) which will likely result in some CNT aggregates/bundles less tightly bound within the mat. For backwashing times in excess of ≈10 min, however, Fig. 4 shows that the quantity of CNTs removed by backwashing with Milli-Q water for all of the HF-PVDF-CNT and HF-PES-CNT membranes was at or below the detection limit ($> 6.6 \times 10^{-5}$ mg MWCNT). For all of the HF-PVDF-CNT and HF-PES-CNT membranes the total mass of MWCNTs lost from the mats during long term backwashing with Milli-Q water was < 50 μg, as compared to the approximately 10 mg MWCNTs used to create them (< 0.5% of the total MWCNT mass used in the loading process).

For the majority of the membranes tested the quantity of MWCNTs released during the hydraulic stress steps was below the detection limit even for really high water fluxes (i.e. 420 L h^{-1} m^{-2}). However, one of the HF-PES-CNT membranes did lose greater quantities of MWCNTs during each of the hydraulic stress steps (see Fig. 4). The extent of CNT loss from this HF-PES-CNT membrane in several different backwashing steps is shown visually in the backwashed water collected (see Fig. S5), demonstrating that even in this case the vast majority of the CNTs were retained on the membrane's inner surface. In general, the

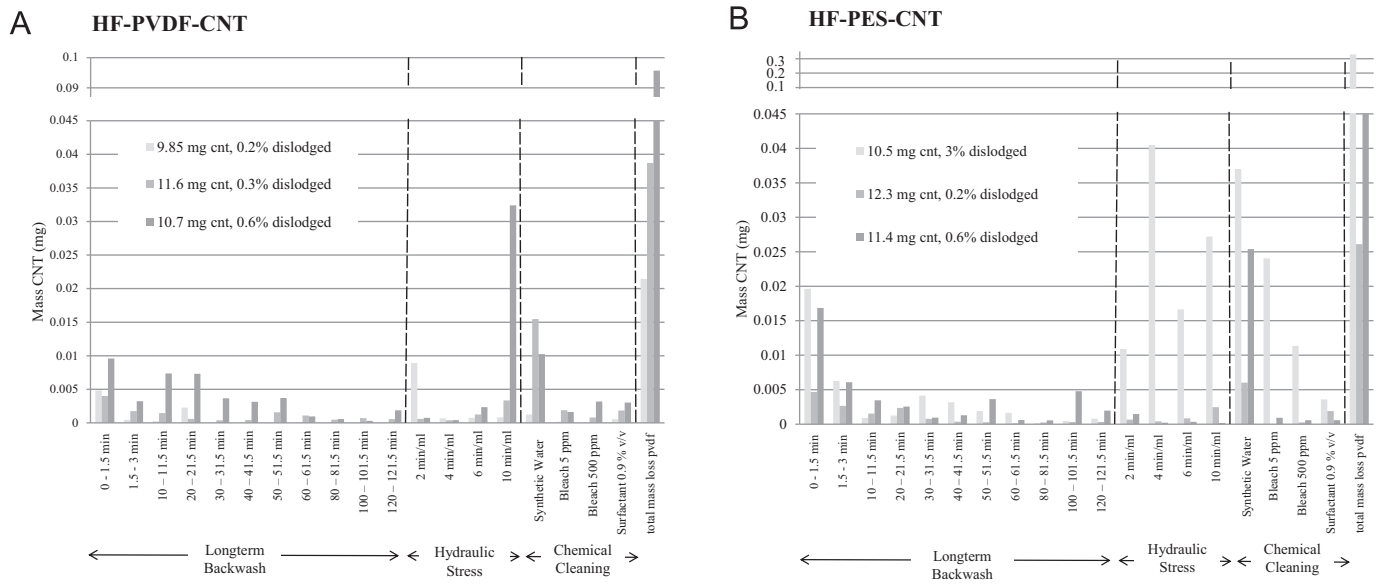

Fig. 4. Mass of MWCNTs released from HF-PVDF-CNT (A) and HF-PES-CNT (B) membranes during a sequence of backwashing steps where the flow direction was reversed (i.e. from the "outside in"). Results are shown for experiments performed on three different HF-PVDF-CNT and HF-PES-CNT membranes. The backwashing steps consisted of (in order) prolonged backwashing with Milli-Q water, hydraulic stress with Milli-Q water and finally chemical cleaning (see text for details). During each step the mass of CNTs released was determined by UV–vis analysis of the backwash (see text for details).

quantity of CNTs removed during each one of the different chemical treatment steps was small (<0.05 mg); the most disruptive treatment was the backwash with the synthetic water solution at a flux of 85 L h^{-1} m^{-2}.

Based on the total mass of MWCNTs lost during the entire sequence of backwashing steps it is evident that the MWCNT mats formed on the HF-PVDF-CNT and HF-PES-CNT membranes remain intact after backwashing and chemical cleaning. For five of the six HF-PVDF-CNT and HF-PES-CNT membranes tested, $<1\%$ of the initial MWCNT mass used to create the mats was lost. In general, HF-PVDF-CNT and HF-PES-CNT membranes exhibited comparable stabilities which suggest that mat's stability is more a consequence of its structure than a result of specific CNT interactions with the membrane surface.

Cross-sectional SEM images of the HF-PVDF-CNT (Fig. 5A; HF-PVDF) and HF-PES-CNT (Fig. 5B; HF-PES) membranes acquired after the backwashing steps provide visual confirmation that CNT mats are still present on the membrane's inner surface. In addition to the obvious retention of the CNTs, the lower magnification SEM images (Fig. 5, A1 and B1) also reveal that the CNT mats are formed continuously around the inner surface of the hollow fiber membranes with a relatively uniform thickness. The higher resolution electron micrographs (Fig. 5A2 and B2) also highlight the similar thickness of the CNT mat before and after backwashing (compare Fig. 3A and B) and the abrupt nature of the interface that still exists between the CNT mat and the base membrane (HF-PVDF or HF-PES).

The robustness of the HF-PVDF-CNT and HF-PES-CNT mats created on the inner surface of the membranes contrasts with the instability of CNTs mats deposited on the outer surface of the same membrane. Thus, a visible darkening of the solution in the membrane module (Fig. S6) demonstrates that even simple backwashing from the inside-out removed large quantities of CNTs deposited on the outer surface of a HF-PVDF membrane. This observation is consistent with our previous findings that CNT mats adsorbed on flat sheet membranes are easily removed by simple backwashing with Milli-Q water [32]. In contrast, backwashed samples collected when the CNT mats were deposited on the inner surfaces of the hollow fiber membranes were colorless to the naked eye, indicative of a dramatically greater stability.

3.3. Evaluation of CNT mobilization during filtration of humic substances

In addition to ensuring CNTs remain intact during backwashing, it is also important to confirm that CNTs do not break through the membrane and enter the permeate during inside-out water filtration (i.e. regular use). Any breakthrough of CNTs during filtration would raise important safety issues as CNTs could enter the treated water where their environmental health and safety effects remain unresolved and are the topic of intense scientific debate [51].

Humic substances exhibit a strong propensity for facilitated transport and for stabilizing CNTs as suspended particles [52], and SRNOM filtration is thus a stringent test for CNT stability. To simulate conditions most likely to facilitate CNT transport through the membrane, (1) the membrane pore size should be relatively large and, (2) the SRNOM should not induce fouling which would decrease the membrane's effective pore size and thus the propensity for CNT transport. To address the first issue we chose to study the HF-PVDF membrane because of its larger pore size (0.1 μm for HF-PVDF vs. 0.03 μm for HF-PES) as compared to the CNT dimensions (lengths of 10–20 μm with outer diameters of 50–80 nm). To address the second issue, SRNOM (<800 Da determined by HPLC-SEC with DOC detection) was chosen because the molecular weight of SRNOM is small enough so that no fouling would be expected during SRNOM filtration through the HF-PVDF membrane.

During SRNOM filtration the UV absorbance in the 800–900 nm range of all permeate samples were below the MWCNT detection limit (0.011 absorbance units, Table S1). The TMP also remained constant indicating a lack of organic fouling as expected (Fig. S7). UV analysis of the backwash conducted at the end of the SRNOM filtration cycle using the permeate (85 L h^{-1} m^{-2}) revealed the presence of ≈10 μg MWCNTs. Thus, our results demonstrate that within our detection limits no facilitated CNT transport occurred

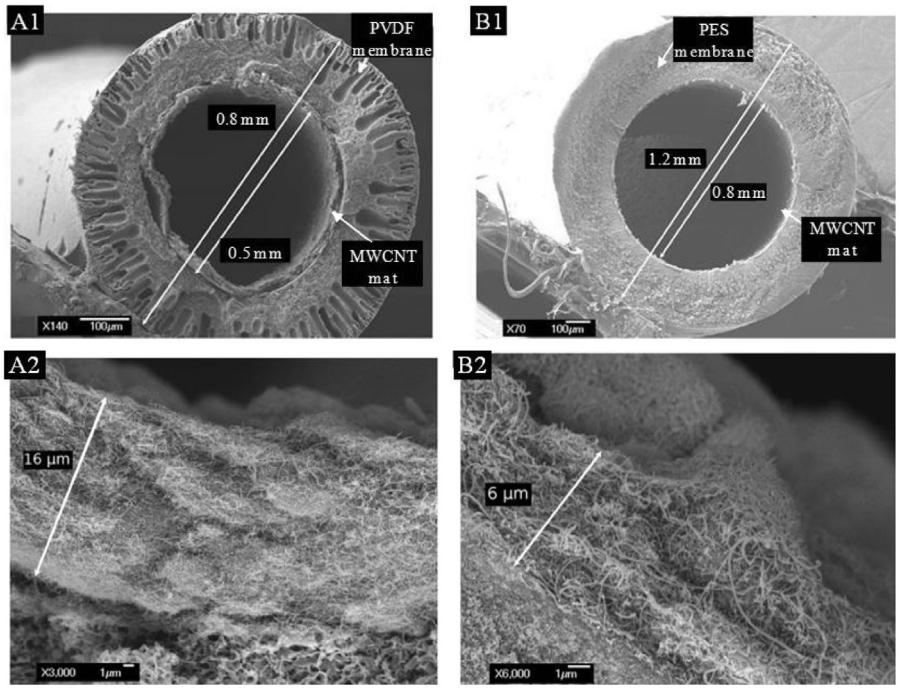

Fig. 5. SEM pictures of MWCNT mats on the inner surface of PVDF (A1 and A2) and PES (B1 and B2) hollow fiber membranes after the membranes were backwashed. A1 and B2 are zoomed out SEM images that show the cross section of the modified hollow fibers. A2 and B2 SEM images show the detailed nature of the membrane/MWCNT interface.

through the HF-PVDF-CNT membrane during inside-out SRNOM filtration, although a small quantity of MWCNTs were removed during backwashing, consistent with our results in Section 3.2 on the mat's stability. These findings support the idea that CNT mats created on the inner surfaces of hollow fiber membranes can be used without introducing unwanted CNTs into the permeate.

3.4. Effectiveness and stability of MWCNT mats during alginate filtration

As previously reported [32] CNT mats created on flat sheet PVDF membranes can reduce membrane fouling. In the present study, the fouling resistance of HF-PVDF-CNT and HF-PES-CNT membranes was tested by monitoring the change in TMP during the filtration of sodium alginate, a typical fouling surrogate used in membrane studies. It should be noted that this study is distinct from the one previously described in Section 3.3 which was designed specifically to evaluate the potential for any CNT remobilization during filtration of NOM. In contrast, sodium alginate represents a far more aggressive foulant enabling us to evaluate the benefits that CNT mats have on fouling resistance, including their ability to sustain any improvements through repeated backwashing steps.

Fig. 6 shows a representative example of the TMP increase measured as a function of time during alginate filtration for the two membrane types. Regardless of the membrane, the TMP variation showed two regimes described by a rapid increase in TMP followed by a slower, more linear rate of increase. This could be a reflection of different fouling mechanisms (such as pore blockage and cake filtration for the first and second steps, respectively) [53], although a detailed study as to reasons why CNT mats increased the fouling resistance of the membranes was not the focus of the present study. As a convenient metric to compare the fouling resistance of different membranes we used the rate of TMP increase in the second regime (the linear increase in TMP observed towards the end of each cycle).

Fig. 6-A shows that during each cycle of alginate filtration the rate of TMP increase for the HF-PVDF-CNT membranes decreased considerably compared to the HF-PVDF membranes. Thus, for the HF-PVDF and HF-PVDF-CNT membranes the fouling rate in the first cycle was equal to 2 and 0.8 mbar min^{-1}, respectively. Consequently, the presence of a CNT mat reduced the fouling rate by about 60%. The improvement in the antifouling properties of the HF-PVDF-CNT membranes were sustained through all four filtration cycles and backwashing steps with the final TMP after ≈5 h equal to 0.3 and 0.1 bars for the HF-PVDF and HF-PVDF-CNT membranes, respectively. The observation that the fouling resistance of the HF-PVDF-CNT membranes was sustained through repeated backwashing steps, shown in Fig. 6-A, is further evidence that the CNT mats remain intact on the membrane's inner surface. As shown in Fig. 6-A the presence of CNT mats also decreased the extent of irreversible fouling. Before fouling the permeability of the HF-PVDF and HF-PVDF-CNT membranes was 655 ± 85 and 434 ± 52 L h^{-1} m^{-2} bar^{-1}; after the last backwash step permeabilities had decreased to 468 ± 56 and 395 ± 43 L h^{-1} m^{-2} bar^{-1}, respectively. Thus, the irreversible fouling reduced the permeability of the HF-PVDF membranes by 29% but the HF-PVDF-CNT membrane by only 9%.

The CNT mats were, however, much less effective at reducing alginate fouling when adsorbed on the inner surface of PES membranes. During the first cycle the fouling rate was 2 and 1.3 mbar $min^{-1}$for the HF-PES and HF-PES-CNT membranes, respectively. Furthermore, after each filtration cycle the relative improvement of the HF-PES-CNT membrane compared to the HF-PES membrane decreased such that after three backwash cycles the performance of the HF-PES-CNT and the HF-PES membrane were virtually indistinguishable from one another. The extent of irreversible fouling was negligible for either the HF-PES-CNT membrane or the HF-PES membrane.

The reason why the CNT mats have a greater effect on the performance of the HF-PVDF membranes compared to the HF-PES membrane can be ascribed to the difference in pore-size between the two types of hollow fiber membranes and the CNT mats.

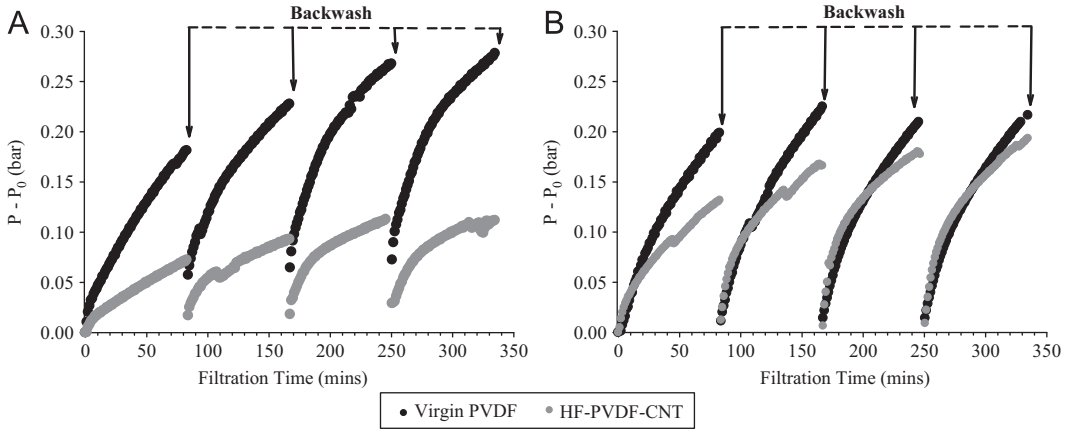

Fig. 6. TMP increase (P–P_0) during the filtration of a 5 ppm alginate suspension through (A) PVDF and (B) PES virgin and MWCNT modified hollow fiber membranes. The flux of alginate was held constant at 67 L h^{-1} m^{-2}. The vertical arrows indicate times at which the membrane was backwashed with the permeate at 134 L h^{-1} m^{-2}. Data is shown for four cycles of 80 min filtration followed by 6 min backwashes.

The HF-PES and HF-PVDF membranes have pore sizes of <0.03 μm and ≈0.1 μm, respectively, while the CNT mats have a pore size distribution predominantly in the range 0.01–0.1 μm based on our previous findings with flat sheet membranes [32]. Thus, for the HF-PVDF membrane the CNT mat introduces a new, finer filter that helps to trap the particles responsible for clogging/blocking membrane pores. In contrast, the pore size in the HF-PES membrane is comparable to the pore size in the CNT mat. Consequently, the CNT mat produces far less of a change in the membrane's antifouling properties. The exact mechanism of fouling reduction by CNT mats is currently under investigation.

3.5. Rationalizing the CNT mat stability

The central finding of this study is that backwashable CNT mats can be generated on the inner surfaces of hollow fiber membranes using a simple preparative method. Our working hypotheses is that the detailed nature of membrane–CNT interactions is not playing a major role in determining the mat's stability due to our ability to create stable CNT mats on two membranes (HF-PVDF and HF-PES) with very different physicochemical properties (different hydrophilic properties, pore size, chemical composition, etc.).

To explore the generalizability of a mat's stability on the inner surface of a hollow fiber membrane we conducted a limited number of experiments using powder activated carbon (PAC) (200–400 mesh; 75–35 micron), rather than CNTs. In these studies, surfactant stabilized particles of powder activated carbon (PAC) were filtered through a HF-PVDF membrane from the inside-out using an experimental approach analogous to the one used for CNTs. During the loading procedure a qualitatively similar variation in TMP was observed. Thus, at the end of the PAC loading step and subsequent flushing of the surfactant with Milli-Q water the measured TMP was similar to that of the virgin membrane. Two HF-PVDF-PAC membrane modules were created in this way, with loadings of ≈19 g cm^{-2} and ≈28 g cm^{-2}. Both membranes were then subjected to prolonged backwashing with Milli-Q water and hydraulic stress as described in Section 2.2 (i) and (ii). Visual analysis of the backwashed water showed that the vast majority of the PAC had been retained within the membranes. This was confirmed by SEM analysis, which showed that PAC mats remained on the inner surface of the HF-PVDF (see Fig. S8). This result indicates that the stability of the CNT mats, which are the focus of this investigation, is not a consequence of the unique physicochemical properties of CNTs but is a more generalizable phenomenon that can likely be extended to a range of other materials.

Thus, a key question is why are the mats created on the inner surface of the hollow fiber membranes stable to aggressive backwashing, while mats deposited either on flat sheet membranes or on the outer surface of hollow fiber membranes are easily removed by the most simple backwashing steps? [35,36]. As a first step towards rationalizing this phenomenon it is constructive to consider the stresses that mats experience during backwashing as a result of the water pressure. Based on the SEM images shown in Fig. 5 the CNT mats can be considered as a thin walled cylinder since their thickness is less than 1/20 of their diameter [54]. As stated previously by Brinket et al. [55] hollow fibers, and therefore by inference the CNTs mats, will be mainly subjected to radial and circumferential stresses during filtration, although longitudinal stress can be neglected as the fiber is open on one end. During backwashing the greatest stress experienced by a mat loaded on the outer surface of fiber is tensile hoop stress which exerts a force that tries to expand the material [56]. In contrast, a mat created on inner surface of a fiber is subjected to compressive hoop stresses. Thus, our results suggest that the difference in mat stability is related principally to the nature and directionality of stresses that they experience during backwashing (compressive or tensile) with mats being more resistant to compressive as opposed to tensile forces. Indeed, for a given material its compressive strength is generally higher than its tensile strength [57]. Moreover, the magnitude of the stresses experienced by the mat during backwashing depend on the diameter of the mat; CNT mats created on the outer surface will be subjected to higher stress because they exhibit larger diameters than ones created on the inner surface. Thus, both the nature and magnitude of the forces both point towards a greater stability for CNT mats created on the inner surface of hollow fibers and subjected to outside-in backwashing. Further theoretical studies and computational modeling will be necessary to fully explore the reasons for the mat's stability.

4. Conclusions

We describe a new and simple method to generate backwashable CNT mats on the inner surface of hollow fiber polymeric membranes. The method involves filtering a CNT suspension through a hollow fiber membrane operating in dead-end mode from the inside-out. The most impressive attribute of these CNT mats is their ability to withstand backwashing, including long term backwashing and hydraulic stress with Milli-Q water and chemical cleaning, while maintaining permeability. On average, the CNT mats lost $<1\%$ of their initial mass during these

backwashing steps; the mat's stability was confirmed visually by cross-sectional SEM images taken before and after backwashing. The stability of CNT or PAC mats created on the inner surface of hollow fiber membranes is in marked contrast to the facile release of CNTs from mats created on the outer surface of hollow fiber membranes or on flat sheet membranes towards even the simplest and least aggressive backwash steps. This difference in stability is ascribed to differences in the nature and directionality of the forces that the mats experience during backwashing rather than any differences in the intrinsic properties of the materials used to create the mats. The potential for CNT mats to enhance hollow fiber membrane performance in real world applications is highlighted by their ability to sustainably improve the antifouling resistance of HF-PVDF membranes through several filtration/cleaning steps. However, the potential applications of the CNT mats described in this study only apply to hollow fiber membranes being operated in an inside out mode.

Acknowledgments

The authors would like to thank Mr. Mark Koontz and David Goodwin for the SEM images, Jin Yang for UV–vis method development, and Gaurav Ajmani and Dr. Joseph Jacangelo for valuable discussions during the studies. This research was partially supported by the Region Poitou-Charentes of France and from a SEED grant administered by the Environment, Energy, Sustainability and Health Institute (E2HSI) of the Johns Hopkins University (JHU). Additional funding was also provided by the JHU Global Water Program and the Osprey Foundation of Maryland.

Appendix A. Supporting information

Supplementary data associated with this article can be found in the online version at http://dx.doi.org/10.1016/j.memsci.2013.06.015.

References

[1] J.M. Schnorr, T.M. Swager, Emerging applications of carbon nanotubes, Chem. Mater. 23 (2010) 646–657.
[2] M. Paradise, T. Goswami, Carbon nanotubes – production and industrial applications, Mater. Des. 28 (2007) 1477–1489.
[3] S.R. Corrie, R. Vogel, I. Keen, K. Jack, D. Kozak, G. Lawrie, B.J. Battersby, P. Fredericks, M. Trau, A structural study of hybrid organosilica materials for colloid-based DNA biosensors, J. Mater. Chem. 18 (2008) 523–529.
[4] N. Savage, M.S. Diallo, Nanomaterials and water purification: opportunities and challenges, J. Nanoparticle Res. 7 (2005) 331–342.
[5] M.R. Wiesner, Responsible development of nanotechnologies for water and wastewater treatment, Water Sci. Technol. 53 (2006) 45–51.
[6] X. Ren, C. Chen, M. Nagatsu, X. Wang, Carbon nanotubes as adsorbents in environmental pollution management: a review, Chem. Eng. J. 170 (2011) 395–410.
[7] A.V. Herrera-Herrera, M.Á. González-Curbelo, J. Hernández-Borges, M.Á. Rodríguez-Delgado, Carbon nanotubes applications in separation science: a review, Anal. Chim. Acta 734 (2012) 1–30.
[8] B. Karn, T. Kuiken, M. Otto, Nanotechnolgy and in situ remediation: a review of the benefits and potential risks, Environ. Health Perspect. 117 (2009) 1823–1831.
[9] T.C. Zhang, R.Y. Surampalli, K.C.K. Lai, Z. Hu, R.D. Tyagi, I.M.C. Lo, Nanotechnologies for Water Environment Applications, American Society of Civil Engineers, Reston, VA, 2009.
[10] C. Lu, H. Chiu, Adsorption of zinc(II) from water with purified carbon nanotubes, Chem. Eng. Sci. 61 (2006) 1138–1145.
[11] Y.-H. Li, S. Wang, Z. Luan, J. Ding, C. Xu, D. Wu, Adsorption of cadmium(II) from aqueous solution by surface oxidized carbon nanotubes, Carbon 41 (2003) 1057–1062.
[12] C. Chen, X Wang, Adsorption of Ni(II) from aqueous solution using oxidized multiwall carbon nanotubes, Ind. Eng. Chem. Res. 45 (2006) 9144–9149.
[13] H.H. Cho, B.A. Smith, J.D. Wnuk, D.H. Fairbrother, W.P. Ball, Influence of surface oxides on the adsorption of naphthalene onto multiwalled carbon nanotubes, Environ. Sci. Technol. 42 (2008) 2899–2905.
[14] H.H. Cho, K. Wepasnick, B.A. Smith, F.K. Bangash, D.H. Fairbrother, W.P. Ball, Sorption of aqueous Zn[II] and Cd[II] by multiwall carbon nanotubes: the relative roles of oxygen-containing functional groups and graphenic carbon, Langmuir 26 (2010) 967–981.
[15] H. Li, X. Gui, L. Zhang, S. Wang, C. Ji, J. Wei, K. Wang, H. Zhu, D. Wu, A. Cao, Carbon nanotube sponge filters for trapping nanoparticles and dye molecules from water, Chem. Commun. (Cambridge, UK) 46 (2010) 7966–7968.
[16] J. Heo, L. Joseph, Y. Yoon, Y.G. Park, N. Her, J. Sohn, S.H. Yoon, Removal of micropollutants and NOM in carbon nanotube-UF membrane system from seawater, Water Sci. Technol. 63 (2011) 2737–2744.
[17] C.D. Vecitis, G. Gao, H. Liu, Electrochemical carbon nanotube filter for adsorption, desorption, and oxidation of aqueous dyes and anions, J. Phys. Chem. C 115 (2011) 3621–3629.
[18] T. Mohammadi, M.A. Tofighy, Adsorption of divalent heavy metal ions from water using carbon nanotube sheets, J. Hazard. Mater. 185 (2011) 140–147.
[19] O. Moradi, The removal of ions by functionalized carbon nanotube: equilibrium, isotherms and thermodynamic studies, Chem. Biochem. Eng. Q 25 (2011) 229–240.
[20] D.S. Su, Y.J. Xu, R. Arrigo, X. Liu, Characterization and use of functionalized carbon nanotubes for the adsorption of heavy metal anions, New Carbon Mater. 26 (2011) 57–62.
[21] O. Moradi, K. Zare, M. Monajjemi, M. Yari, H. Aghaie, The studies of equilibrium and thermodynamic adsorption of Pb(II), Cd(II) and Cu(II) ions from aqueous solution onto SWCNTs and SWCNT-COOH surfaces, fullerenes, nanotubes, Carbon Nanostruct. 18 (2010) 285–302.
[22] X.K. Wang, C.L. Chen, J. Hu, D.D. Shao, J.X. Li, Adsorption behavior of multiwall carbon nanotube/iron oxide magnetic composites for Ni(II) and Sr(II), J. Hazard. Mater. 164 (2009) 923–928.
[23] A.S. Brady-Estévez, T.H. Nguyen, L. Gutierrez, M. Elimelech, Impact of solution chemistry on viral removal by a single-walled carbon nanotube filter, Water Res. 44 (2010) 3773–3780.
[24] S.T. Mostafavi, M.R. Mehrnia, A.M. Rashidi, Preparation of nanofilter from carbon nanotubes for application in virus removal from water, Desalination 238 (2009) 271–280.
[25] S. Kang, M.S. Mauter, M. Elimelech, Single walled carbon nanotubes exhibit strong antimicrobial activity, Environ. Sci. Technol. 43 (2009) 2648–2653.
[26] C.D. Vecitis, M.H. Schnoor, M.S. Rahaman, J.D. Schiffman, M. Elimelech, Electrochemical multiwalled carbon nanotube filter for viral and bacterial removal and inactivation, Environ. Sci. Technol. 45 (2011) 3672–3679.
[27] A. Tiraferri, C.D. Vecitis, M. Elimelech, Covalent binding of single-walled carbon nanotubes to polyamide membranes for antimicrobial surface properties, ACS Appl. Mater. Interfaces 3 (2011) 2869–2877.
[28] M.S. Rahaman, C.D. Vecitis, M. Elimelech, Electrochemical carbon-nanotube filter performance toward virus removal and inactivation in the presence of natural organic matter, Environ. Sci. Technol. 46 (2012) 1556–1564.
[29] H. Liu, C.D. Vecitis, Reactive transport mechanism for organic oxidation during electrochemical filtration: mass-transfer, physical adsorption, and electron-transfer, J. Phys. Chem. C 116 (2012) 374–383.
[30] G.D. Gao, C.D. Vecitis, Doped carbon nanotube networks for electrochemical filtration of aqueous phenol: electrolyte precipitation and phenol polymerization, ACS Appl. Mater. Interfaces 4 (2012) 1478–1489.
[31] G. Gao, C.D. Vecitis, Electrochemical carbon nanotube filter oxidative performance as a function of surface chemistry, Environ. Sci. Technol. 45 (2011) 9726–9734.
[32] G.S. Ajmani, D. Goodwin, K. Marsh, D.H. Fairbrother, K.J. Schwab, J.G. Jacangelo, H. Huang, Modification of low pressure membranes with carbon nanotube layers for fouling control, Water Res. 46 (2012) 5645–5654.
[33] X. Yang, J. Lee, L. Yuan, S.-R. Chae, V.K. Peterson, A.I. Minett, Removal of natural organic matter in water using functionalized carbon nanotube buckypaper, Carbon. 59 (2013) 160–166.
[34] ⟨http:/www.nanotechproject.org⟩, The Project on Emerging Nanotechnologies; Woodrow Wilson International Center for Scholars.
[35] L.F. Dumée, K. Sears, J. Schütz, N. Finn, C. Huynh, S. Hawkins, M. Duke, S. Gray, Characterization and evaluation of carbon nanotube Bucky-Paper membranes for direct contact membrane distillation, J. Membr. Sci. 351 (2010) 36–43.
[36] C.F. DeLannoy, D. Jassby, D.D. David, M Wiesner, A highly electrically conductive polymer-multiwalled carbon nanotube nanocomposite membrane, J. Membr. Sci. 415–516 (2012) 718–724.
[37] D. Furukawa, A Global Perspective of Low Pressure Membranes, National Water Research Institute, Fountain Valley, California, 2008.
[38] G.P. Westerhoff, M.A. Thompson, J.C. Vickers, Experiences in the application of microfiltration and ultrafiltration membrane technology in drinking-water treatment, Water Supply14 (1996) 482–486.
[39] K. Majewska-Nowak, I. Kowalska, M. Kabsch-Korbutowicz, Ultrafiltration of aqueous solutions containing a mixture of dye and surfactant, Desalination 198 (2006) 149–157.
[40] H. Huang, K. Schwab, J.G. Jacangelo, Pretreatment for low pressure membranes in water treatment: a review, Environ. Sci. Technol. 43 (2009) 3011–3019.
[41] C. Jucker, M.M. Clark, Adsorption of aquatic humic substances on hydrophobic ultrafiltration membranes, J. Membr. Sci. 97 (1994) 37–52.
[42] G. Amy, J. Cho, Interactions between natural organic matter (NOM) and membranes: rejection and fouling, Water Sci. Technol. 40 (1999) 131–139.
[43] H. Huang, N. Lee, T. Young, G. Amy, J.C. Lozier, J.G. Jacangelo, Natural organic matter fouling of low-pressure, hollow-fiber membranes: effects of NOM source and hydrodynamic conditions, Water Res. 41 (2007) 3823–3832.

[44] E. Filloux, H. Gallard, J.-P. Croue, Identification of effluent organic matter fractions responsible for low-pressure membrane fouling, Water Res. 46 (2012) 5531–5540.
[45] B. Smith, K. Wepasnick, K.E. Schrote, A.R. Bertele, W.P. Ball, C. O'Melia, D.H. Fairbrother, Colloidal properties of aqueous suspensions of acid-treated, multi-walled carbon nanotubes, Environ. Sci. Technol. 43 (2009) 819–825.
[46] N. Her, G. Amy, H.-R. Park, M. Song, Characterizing algogenic organic matter (AOM) and evaluating associated NF membrane fouling, Water Res. 38 (2004) 1427–1438.
[47] W.-Y. Ahn, A.G. Kalinichev, M.M. Clark, Effects of background cations on the fouling of polyethersulfone membranes by natural organic matter: experimental and molecular modeling study, J. Membr. Sci. (2008) 128–140.
[48] Y. Ye, P. Le Clech, V. Chen, A.G. Fane, B. Jefferson, Fouling mechanisms of alginate solutions as model extracellular polymeric substances, Desalination 175 (2005) 7–20.
[49] K. Katsoufidou, S.G. Yiantsios, A.J. Karabelas, Experimental study of ultrafiltration membrane fouling by sodium alginate and flux recovery by backwashing, J. Membr. Sci. 300 (2007) 137–146.
[50] A.-S. Jönsson, B. Jönsson, The influence of nonionic and ionic surfactants on hydrophobic and hydrophilic ultrafiltration membranes, J. Membr. Sci. 56 (1991) 49–76.
[51] J.M. Wörle-Knirsch, K. Pulskamp, H.F. Krug, Oops they did it again! Carbon nanotubes hoax scientists in viability assays, Nano Lett. 6 (2006) 1261–1268.
[52] M.A. Chappell, A.J. George, K.M. Dontsova, B.E. Porter, C.L. Price, P. Zhou, E. Morikawa, A.J. Kennedy, J.A. Steevens, Surfactant stabilization of multi-walled carbon nanotube dispersions with dissolved humic substances, Environ. Pollut. (Oxford, UK) 157 (2009) 1081–1087.
[53] D.M. Kanani, X. Sun, R. Ghosh, Reversible and irreversible membrane fouling during in-line microfiltration of concentrated protein solutions, J. Membr. Sci. 315 (1–2) (2008) 1–10.
[54] M. Mory, Fluid Mechanics for Chemical Engineering, University of Pau and the Adour Region, France.
[55] L. Brinkert, N. Abidine, P. Aptel, On the relation between compaction and mechanical properties for ultrafiltration hollow fibers, J. Membr. Sci. 77 (1) (1993) 123–131.
[56] A.J. Gijsbertsen-Abrahamse, E.R. Cornelissen, J.A.M.H. Hofman, Fiber failure frequency and causes of hollow fiber integrity loss, Desalination 194 (1–3) (2006) 251–258.
[57] A. Shukla, G. Ravichandran, Y.D.S. Rajapakse, Dynamic Failure of Materials and Structures, Springer Book 978-1-4419-0446-1.